

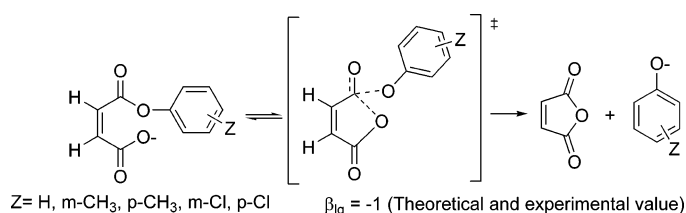
Kinetic and Theoretical Studies on the Mechanism of Intramolecular Catalysis in Phenyl Ester Hydrolysis

Gabriel O. Andrés, Adriana B. Pierini,* and Rita H. de Rossi*

*Instituto de Investigaciones en Físico Química de Córdoba (INFIQC), Facultad de Ciencias Químicas
Departamento de Química Orgánica, Universidad Nacional de Córdoba, Ciudad Universitaria,
5000 Córdoba, Argentina*

adriana@mail.fcq.unc.edu.ar; ritah@fcq.unc.edu.ar

Received June 7, 2006



The kinetic study of the hydrolysis reaction of Z-substituted phenyl hydrogen maleates (Z = H, *m*-CH₃, *p*-CH₃, *m*-Cl, *p*-Cl and *m*-CN) was carried out in aqueous solution, and the results were complemented with theoretical studies. Under some experimental conditions, two kinetic processes were observed. One of them was ascribed to maleic anhydride formation and the other to the anhydride hydrolysis. The Brønsted-type plot for the leaving-group dependence was linear with slope β_{lg} = -1. The experimental results are consistent with a mechanism that involves significant bond breaking in the rate-limiting transition state (α_{lg} = 0.64). Theoretical results for the reaction in the gas phase showed an excellent Brønsted-type dependence with a β_{lg} of -1.03. A tetrahedral intermediate (TI) could not be found through DFT gas-phase studies (B3LYP/6-311+G*). Calculations carried out within a continuous solvation model or with discrete water molecules failed to find a stable TI. With both models, a flat region on the potential-energy surface is found and a tight optimization of the structures led back to starting materials. The theoretical results do not discard the possible existence of an unstable intermediate on the free-energy surface, but the analysis of the whole body of results compared with other acyl transfer reactions lead us to suggest that an enforced concerted mechanism is the most appropriate to describe these reactions.

Introduction

The study of enzymatic hydrolysis is of great interest because the rate enhancement can be quite dramatic.^{1,2} Intramolecular catalysis has been used as a model system that gives important information about enzyme mechanisms.³⁻⁷ The efficiency of the reactions is very much dependent on the relative position of the reacting groups⁸ and the time they spend at the proper distance for reaction.⁹ The last point was elegantly proved by

computational studies that show that the rate of an intramolecular reaction is proportional to the time that the catalytic group and the reaction center reside at a critical distance.¹⁰⁻¹³ These calculations are in good agreement with Menger's "spatiotemporal" hypothesis¹⁴ and shed light on different questionable aspects regarding the mechanism of enzymatic catalysis.

Ester hydrolysis is an important type of reaction that has received a great deal of attention in both organic chemistry and biochemistry, and it has been subjected to many investigations.¹⁵⁻¹⁹

(1) Jencks, W. P. *Catalysis in Chemistry and Enzymology*; Dover: U.S.A., 1969.

(2) Wolfenden, R.; Zinder, M. J. *Acc. Chem. Res.* **2001**, *34*, 938.

(3) Kirby, A. J.; Dutta-Roy, N.; da Silva, D.; Goodman, J. M.; Lima, M. F.; Roussev, C. D.; Nome, F. *J. Am. Chem. Soc.* **2005**, *127*, 7033.

(4) Fife, T. H.; Singh, R.; Bembli, R. *J. Org. Chem.* **2002**, *67*, 3179.

(5) Menger, F. M.; Ladina, M. *J. Am. Chem. Soc.* **1988**, *110*, 6794.

(6) Suh, J.; Chun, K. H. *J. Am. Chem. Soc.* **1986**, *108*, 305.

(7) Kirby, A. J.; Lancaster, P. W. *J. Chem. Soc., Perkins Trans. 2* **1972**, 1206.

(8) Bond, A. D.; Kirby, A. J.; Rodriguez, E. *Chem. Commun.* **2001**, 2266.

(9) Menger, F. M.; Fei, Z. X. *Angew. Chem., Int. Ed. Engl.* **1994**, *33*, 346.

(10) Lightstone, F. C.; Bruice, T. C. *Acc. Chem. Res.* **1999**, *32*, 127.

(11) Lightstone, F. C.; Bruice, T. C. *Bioorg. Chem.* **1998**, *26*, 193.

(12) Lightstone, F. C.; Bruice, T. C. *J. Am. Chem. Soc.* **1997**, *119*, 9103.

(13) Lightstone, F. C.; Bruice, T. C. *J. Am. Chem. Soc.* **1996**, *118*, 2595.

(14) Menger, F. M. *Acc. Chem. Res.* **1985**, *18*, 128.

(15) Marlier, J. F. *Acc. Chem. Res.* **2001**, *34*, 283.

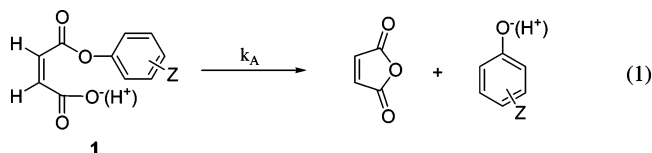
(16) Um, I.-H.; Back, M.-H.; Han, H.-J. *Bull. Korean Chem. Soc.* **2003**, *24*, 1245.

Since the 1950s, it has been widely accepted that the hydrolysis of alkyl esters occurs via a stepwise addition–elimination mechanism.^{20,21} The nucleophilic attack of the hydroxide ion on the acyl carbon gives as a result a stable oxyanion tetrahedral intermediate (TI), which in a subsequent step collapses to form products.²² Indirect experiments^{20,23} and theoretical evidence^{24–26} of TI existence are quite convincing, and the mechanism of nucleophilic displacement on acyl derivatives in solution has been explained by the concept of a stable intermediate. On the other hand, for good leaving groups such as aryloxy ions, there is reasonably good evidence that acyl transfer reactions proceed through concerted mechanisms, where the nucleophilic attack and leaving group departure occur simultaneously and a TI is not formed along the reaction coordinate.^{27–30} All these studies pertain to intermolecular reactions,^{27,31,32} but the subject was only seldom discussed for intramolecular reactions.³³

In previous work we have reported that the hydrolysis reactions of phthalic acid monoesters are strongly sensitive to the pK_a of the phenol leaving group ($\beta_{lg} = -1.15$),³³ which indicates a significant bond breaking in the transition state of the rate determining step. Besides from a study of the back reaction, that is, the phenolysis of phthalic and maleic anhydride, we concluded that the results were consistent with a concerted or enforced concerted mechanism.³⁴

Although linear-free relationships is one of the most useful techniques for the study of mechanisms,²⁷ it is not always enough to distinguish between concerted and stepwise pathways.

We report here experimental and theoretical results for the hydrolysis of aryl hydrogen maleates **1**, which are important for the relevant discussion about the concerted versus the stepwise mechanism on intramolecularly catalyzed ester hydrolysis.

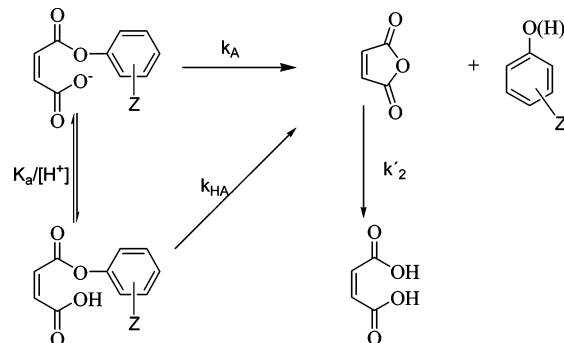


- (17) Frago, A.; Cao, R.; Baños, M. *Tetrahedron Lett.* **2004**, *45*, 4069.
 (18) Hengge, A. C.; Hess, R. A. *J. Am. Chem. Soc.* **1994**, *116*, 11256.
 (19) Hawins, M. D. *J. Chem. Soc., Perkins Trans.* **2 1975**, 285.
 (20) Bender, M. L. *J. Am. Chem. Soc.* **1951**, *73*, 1626.
 (21) Bender, M. L. *Chem. Rev.* **1960**, *60*, 53.
 (22) Carroll, F. A. *Perspectives on Structure and Mechanism in Organic Chemistry*; Brooks/Cole Publishing Company: St. Paul, MN, 1998.
 (23) Kellogg, B. A.; Brown, R. S. *J. Am. Chem. Soc.* **1995**, *117*, 1731.
 (24) Topf, M.; Richards, W. G. *J. Am. Chem. Soc.* **2004**, *126*, 14631.
 (25) Zhan, C. G.; Landry, D. W.; Ornstein, R. L. *J. Am. Chem. Soc.* **2000**, *122*, 1522.
 (26) Pliego, J. R.; Riveros, J. M. *Chem. Eur. J.* **2002**, *8*, 1945.
 (27) Williams, A. *Free Energy Relationship in Organic and Bio-Organic Chemistry*; The Royal Society of Chemistry: Cambridge, U.K., 2003.
 (28) Ba-Saif, S.; Maude, A. B.; Williams, A. *J. Chem. Soc., Perkin Trans. 2* **1994**, 2395.
 (29) Stefanidis, D.; Cho, S.; Dhe-Paganon, S.; Jencks, W. P. *J. Am. Chem. Soc.* **1993**, *115*, 1650.
 (30) Ba-Saif, S.; Luthra, A. K.; Williams, A. *J. Am. Chem. Soc.* **1987**, *109*, 6362.
 (31) Castro, E. A.; Pavez, P.; Santos, J. G. *J. Org. Chem.* **2002**, *67*, 4494.
 (32) Castro, E. A.; Angel, M.; Pavez, P.; Santos, J. G. *J. Chem. Soc., Perkin Trans. 2* **2001**, 2351.
 (33) Andrés, G. O.; Granados, A. M.; de Rossi, R. H. *J. Org. Chem.* **2001**, *66*, 7653.
 (34) Andrés, G. O.; de Rossi, R. H. *J. Org. Chem.* **2005**, *70*, 1445.

TABLE 1. Rate Constants and Kinetic pK_a s for the Hydrolysis of Aryl Hydrogen Maleates **1^a**

Z	pK_a^b	k_{HA}^c 10^{-2} s^{-1}	k_A^c 10^{-2} s^{-1}	k_N^d $10^4 \text{ s}^{-1} \text{ M}^{-1}$	K_e^e 10^5 M^{-1}
<i>p</i> -CH ₃	3.03 ± 0.06	0.2 ± 0.1	5.5 ± 0.1	23	42 (46)
<i>m</i> -CH ₃	3.0 ± 0.1	0.3 ± 0.2	8.0 ± 0.2	16.5	20.6
H	3.10 ± 0.09	0.4 ± 0.2	9.7 ± 0.3	10.7	11 (11)
<i>p</i> -Cl	2.68 ± 0.04	0.7 ± 0.6	39.7 ± 0.4	9.6	2.4
<i>m</i> -Cl	2.66 ± 0.05	2 ± 2	90 ± 9	3.65	0.40 (0.37)

SCHEME 1



Results and Discussion

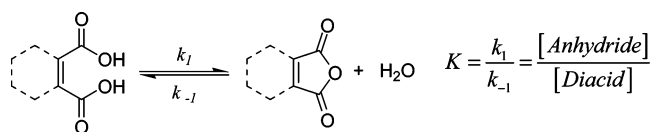
Aryl Hydrogen Maleates. The hydrolysis of aryl hydrogen maleates **1** (Z = H, *p*-Cl, *m*-Cl, *p*-CH₃, *m*-CH₃) were studied between pH 0.60 and 5.60 (Tables S1–S4, Supporting Information). Under some experimental conditions, the kinetics profile showed two kinetics processes: one of them was associated with the anhydride formation and the other with the anhydride hydrolysis (Figure S1). The formation of anhydride as intermediate in these types of reactions is widely known.^{35,36} At a pH higher than 5.60, the kinetics were not measured because the second-order rate constant for the maleic anhydride phenolysis is around 10^4 – $10^5 \text{ s}^{-1} \text{ M}^{-1}$,³⁴ so a little fraction of phenoxide formed at the beginning, make the back reaction of eq 1 quite fast. This complicates the kinetics and, therefore, the interpretation of the results.

The rate constant for the anhydride formation did not show an appreciable dependence on the buffer concentration (Tables S3 and S4). The observed rate constant for the anhydride formation plotted versus pH gives a sigmoid curve (Figures S2–S6) similar to that reported in the literature for substituted aryl hydrogen phthalates.^{33,37} The kinetic pK_a s were calculated from the inflection point of these curves. (Table 1).

The observed rate constants were plotted as a function of the fraction of substrate in the carboxylate form, X_A (plot not shown). The intercepts at $X_A = 0$ are named k_{HA} in Table 1, and they were not zero, although they have a high associated error (at least 50%). These values represent the reaction of the neighboring carboxylic group (Scheme 1). This observation contrasts with the results obtained in the study of the hydrolysis of aryl hydrogen phthalates, where the intercepts of similar plots are indistinguishable from zero.³⁴

- (35) Kirby, A. J. *Adv. Phys. Org. Chem.* **1980**, *17*, 183.
 (36) Bruce, T. C.; Pandit, U. K. *J. Am. Chem. Soc.* **1960**, *82*, 5858.
 (37) Thanassi, J. W.; Bruce, T. C. *J. Am. Chem. Soc.* **1966**, *88*, 747.

SCHEME 2



The equilibrium constants (K) for the formation of phthalic^{38,39} and maleic⁴⁰ anhydride from the corresponding diacid (Scheme 2) are 5×10^{-3} and 0.01, respectively. The value of $k_{-1}[\text{H}_2\text{O}]$ (Scheme 2) determined for phthalic anhydride³³ and maleic anhydride⁴¹ are $9.2 \times 10^{-3} \text{ s}^{-1}$ and $2.5 \times 10^{-2} \text{ s}^{-1}$, respectively. From these data, the values of k_1 can be calculated as $4.6 \times 10^{-5} \text{ s}^{-1}$ and $2.5 \times 10^{-4} \text{ s}^{-1}$ for phthalic and maleic acid, respectively. The ratio of the two rate constants indicates that the carboxylic group of maleic acid is about 5.4 times more reactive than that of phthalic acid. This difference in reactivity may be responsible for the fact that the catalysis by the carboxylic neighboring group was not observed in the hydrolysis of aryl hydrogen phthalates, but it was detected for the maleic derivatives.

The rate constants for the catalysis of neighboring carboxylate group (k_A) as well as the equilibrium constant for the reaction (K_e) collected in Table 1 give linear Brønsted-type plots⁴² with reasonable correlation.

The β_{lg} for the anhydride formation was -1.00 ± 0.06 , which implies an important C–O bond breaking in the rate-limiting transition state.⁴³ Similar β_{lg} values were found for intramolecular catalysis of substituted phenyl hydrogen phthalates ($\beta_{\text{lg}} = -1.15$),³³ the aminolysis of 2-substituted benzoates esters ($\beta_{\text{lg}} = -1$),⁴⁴ and for the carbonate catalysis in the hydrolysis of aryl trifluoroacetates ($\beta_{\text{lg}} = -1.15$).⁴⁵

The β_{Eq} value calculated from the plot of $\log K_e$ versus $\text{p}K_a$ of the leaving group was 1.57 ± 0.09 . This value is the same within experimental error as the value previously reported ($\beta_{\text{Eq}} = 1.69$), determined by an independent method,³⁴ and it is also similar to that reported for acyl transfer reactions ($\beta_{\text{Eq}} = 1.7$).⁴⁶

The change in effective charge obtained from the values of β may be used to position the transition state in the reaction map. This can be done by comparing the effective charge for each of the two atoms that take part in bonding changes in the transition state with that of the product; this ratio, α , is called the Leffler index ($\alpha = \beta/\beta_{\text{Eq}}$).²⁷ The α parameter was estimated from $\alpha_{\text{lg}} = \beta_{\text{lg}}/\beta_{\text{Eq}} = -0.64$. If this value is used as a transition state index (relative to the structure of the reactants and product states), then the value of 0.64, measured from the variation of the phenyl substituents, is consistent with 64% bond rupture

(38) Hawkins, M. D. *J. Chem. Soc., Perkin Trans. 2* **1975**, 282.

(39) Hawkins, M. D. *J. Chem. Soc., Perkin Trans. 2* **1975**, 285.

(40) Ebersson, L.; Welinder, H. *J. Am. Chem. Soc.* **1971**, 93, 5821.

(41) Andrés, G. O.; Silva, O. F.; de Rossi, R. H. *Can. J. Chem.* **2005**, 83, 1281.

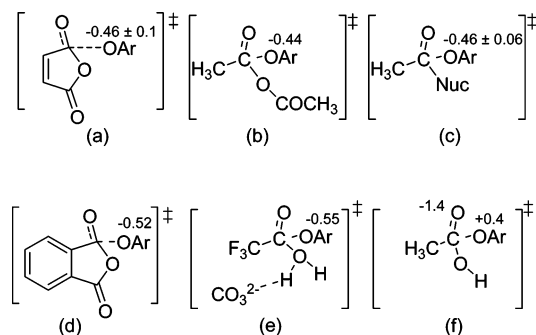
(42) This is not formally a Brønsted plot, and the slope values are not related to general base catalysis. The interaction coefficient (β_{Nuc} , β_{lg} , and β_{Eq}) can be useful for characterizing a reaction mechanism when the change in slope represents a change in the structure of a single transition state. Jencks, W. P. *Chem. Rev.* **1985**, 85, 511.

(43) A referee has pointed out that it is important to consider that β_{lg} do not measure only C–O bond cleavage. Addition to a carbonyl group is very sensitive to substituent effects, so one must expect that a change in aryloxide leaving group will also change the equilibrium constant for addition to the carbonyl forming the TI. This will show up as a nonzero β_{lg} without any bond breaking.

(44) Fiffe, T. H.; Chauffe, L. *J. Org. Chem.* **2000**, 65, 3579.

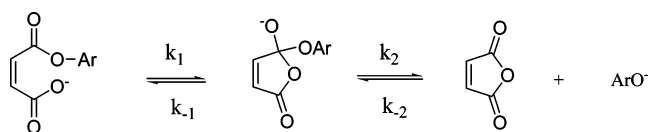
(45) Fernandez, M. A.; de Rossi, R. H. *J. Org. Chem.* **1999**, 64, 6000.

(46) Williams, A. *Acc. Chem. Res.* **1984**, 17, 425.

SCHEME 3^a

^a Key: (a) transition state for the nucleophilic attack of the carboxylate group on the carbonyl ester of aryl hydrogen maleates; (b) transition state for the nucleophilic attack of substituted phenols on acetic anhydride, ref 28; (c) transition state for the reaction of nucleophiles with aryl acetates, ref 29; (d) transition state for the nucleophilic attack of substituted phenols on phthalic anhydride, ref 34; (e) transition state for the hydrolysis of aryl trifluoroacetates, calculated from data in ref 45; and (f) transition state for the hydroxyl attack on aryl esters, ref 27.

SCHEME 4



going from the ester to the anhydride. A value of $\alpha = 0.62$ was obtained in the formation of 2-phenyloxazolin-5-one from aryl benzoyl glycinate, which reacts through a concerted mechanism.⁴⁷

Taking into account the values of β_{Eq} , β_{lg} , and β_{Nuc} , and assuming that the changes in effective charge are conserved, we have estimated the charge on the oxygen in the rate-limiting transition state as -0.46 ± 0.10 ((a) in Scheme 3). Similar effective charges were observed in transition states where a concerted or enforced concerted mechanism was proposed. For example, phenolysis of acetic anhydride ((b) in Scheme 3), nucleophilic attack on aryl acetate esters ((c) in Scheme 3), hydrolysis of aryl trifluoroacetate esters ((e) in Scheme 3), and hydrolysis of aryl acetate esters ((f) in Scheme 3). The charge on oxygen estimated for the intramolecular catalysis on aryl hydrogen maleates and phthalates ((a) and (d) in Scheme 3) are very similar, and also, similarities were found among the values of β . Therefore, it is reasonable to think that the mechanisms are alike and the structure of the transition state for both esters should not be too different.

Linearity of a free-energy plot is not evidence of a mechanism with a single transition state; it indicates that the transition state has a constant structure over the range of substituted phenols employed. A change in the rate-limiting step for the putative stepwise process (Scheme 4) would be expected for a phenol of $\text{p}K_a < 3$,⁴⁸ however, this would be very difficult to measure for two main reasons: (i) the value of k_A would be too high to measure by stopped-flow technique⁴⁹ and (ii) it would be very difficult to synthesize and work with an ester of this type.⁵⁰

(47) Curran, T. C.; Farrar, C. R.; Niaz, O.; Williams, A. *J. Am. Chem. Soc.* **1980**, 102, 6828.

(48) Williams, A. *Chem. Soc. Rev.* **1994**, 94, 93.

(49) Using the value of β_{lg} , we can calculate k_A in the order of $9.4 \times 10^6 \text{ s}^{-1}$ for a leaving group of $\text{p}K_a$ of 2.

Cross correlations can be used to get a better understanding of the intramolecular mechanism, but for the reactions reported here, it is not possible to change the pK_a of the nucleophile, so cross correlations cannot be determined in the usual way. The β_{lg} for esters of substituted phenols that react with nucleophiles by a concerted mechanism change to a more positive value as the pK_a of the nucleophile increases (Figure S8). It is known that the β_{lg} values show a lineal dependence with the pK_a of the nucleophile.^{29,51,52} The existence of this cross correlation is a good indication that there is coupling between the bond-forming and bond-breaking reactions, consistent with a concerted mechanism.

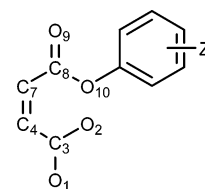
From the cross correlations for intermolecular reactions (Figure S8), a β_{lg} lower than -1 is expected for a nucleophile with $pK_a \approx 3$,⁵³ which is in the range of the experimental value obtained in this work (see above). This result may indicate that the intramolecular reaction is concerted, although this conclusion must be taken with caution because it relies on the assumption that cross correlations from intermolecular reactions are valid for intramolecular ones.

Theoretical Results. To get more insight into the mechanism of the intramolecular reaction, eq 1, we carried out theoretical calculations using ab initio HF and density functional theory methods,⁵⁴ the latter with the hybrid B3LYP functional.⁵⁵ First, the calculations were done for the reactions in the gas phase, and then we inspected the effect on the reaction coordinate of a continuum medium and the addition of discrete water molecules. The semiempirical AM1 procedure was used for a preliminary conformational reactant search. The B3LYP functional was chosen due to its good performance in accounting for electron correlation effects and, therefore, being expected to afford a more appropriate description of the reaction barrier. HF and B3LYP calculations were performed with the 6-311+G* basis set or 6-31+G* when discrete water molecules were used. The inclusion of diffuse functions in the calculations is necessary because of the involvement of anionic species.

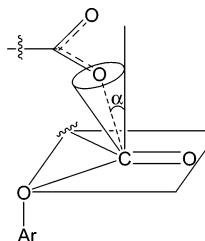
Lightstone and Bruice^{10–13} had determined the importance of the ground-state conformation of the substrate on the rate constant for reactions of several monophenyl esters of carboxylic diacids such as succinic and glutaric. They introduced the term “near attack conformation” (NAC) to define the required conformation for juxtaposed reactants to enter a transition state. The reacting groups of the substrates discussed here belong to the same kind of compounds, but the numbers of starting conformations are more limited and, therefore, the determination of the NAC¹² is much simpler. Using the AM1 method, we explored the different possible conformations that aryl hydrogen maleate esters can adopt. This was carried out by changing the dihedral angle formed between carbons 4, 7, and 8 and the oxygen 10 (Scheme 5). The other relevant dihedrals, $O_9C_8O_{10}C_{Ar}$, $C_8O_{10}C_{Ar}C_{Ar-ortho}$, and $O_2C_3C_4C_7$ were also inspected.

The most stable conformation found has the neighboring carboxylate group in a plane perpendicular to that of the carbonyl ester and in the same plane as the double bond. This

SCHEME 5



SCHEME 6



structure is also a minimum at the HF/6-311+G* and B3LYP/6-311+G* level of theory. It is well-known that the rate of an intramolecular organic reaction is dependent upon the distance between reacting atoms in the starting materials.⁵⁶ The appropriated distances for the intramolecular carboxylate attack of phenyl succinic esters are between 2.8 and 3.2 Å,¹³ for phenyl phthalate ester is 2.7 Å,⁵⁷ and the values calculated in this work for Z-substituted phenyl maleates are 2.55, 2.57, 2.60, and 2.61 Å for Z = *m*-Cl, *p*-Cl, H, and *p*-CH₃, respectively (Figure S9). The rate constants for the intramolecular reactions are $1.42 \times 10^{-3} \text{ s}^{-1}$, $4.43 \times 10^{-2} \text{ s}^{-1}$, and $9.7 \times 10^{-2} \text{ s}^{-1}$ for phenyl hydrogen succinate,³⁵ phthalate,³³ and maleate esters, respectively.

On the other hand, based on data reported in the literature,^{10,58} the approach of the nucleophile had to be within a cone of 30°, with the axis being approximately 17° off the normal to the carbonyl plane (Scheme 6), which is in good agreement with our findings and with the $O_2C_8O_9$ angle of 106–107°, evaluated by HF and B3LYP with the indicated basis set.

The potential surface of minimum energy for the intramolecular carboxylate catalysis on the esters hydrolysis was followed by approaching the oxygen of the neighboring carboxylate group to the carbonyl carbon ester in steps of 0.01 Å.

In doing so, a first transition state (TS1) and the TI were found with HF/6-311+G*. The energy difference between these two states is at most 0.5 kcal/mol (Table 2). Using TI as starting point, the leaving group departure was followed by stretching the bond between the carbonyl carbon of the ester and the oxygen of the phenoxide leaving group until this bond breaks. This inspection led to the localization of the transition state (TS2) whose transition vector corresponds to the departure of the leaving group. The calculated relative energies are summarized in Table 2.

The procedure described was not satisfactory to obtain TS1 and TI with the B3LYP/6-311+G* functional. Instead, a different approach was used, and the minimum energy reaction

(50) The rate constant for the carboxylate intramolecular catalysis of *m*-cyanophenyl hydrogen maleate was obtained from an indirect measurement (ref 34). A direct rate constant value has not been obtained because we were unable to synthesize the ester; it is too unstable.

(51) Jencks, W. P. *Chem. Rev.* **1985**, 85, 511.

(52) Ba-Saif, S.; Luthra, A. K.; Williams, A. *J. Am. Chem. Soc.* **1989**, 111, 2647.

(53) It should be kept in mind that this statement has implied the assumption that the shape of the reaction surface in the proximities of the transition state is independent of the absolute rate of the reactions involved.

(54) (a) Hohenberg, P.; Kohn, W. *Phys. Rev.* **1964**, 136, B864. (b) Kohn, W.; Sham, I. J. *Phys. Rev.* **1965**, 140, A1133.

(55) (a) Lee, C.; Yang, W.; Parr, R. G. *Phys. Rev. B* **1988**, 37, 785. (b) Becke, A. D. *Phys. Rev. A* **1988**, 38, 3098. (c) Miehlich, B.; Savin, A.; Stoll, H.; Preuss, H. *Chem. Phys. Lett.* **1989**, 157, 200.

(56) Scheiner, S. *J. Am. Chem. Soc.* **1981**, 103, 315.

(57) Andres, G. O. Ph.D. Thesis, Universidad Nacional de Cordoba, Argentina, 2004.

(58) Dorigo, A. E.; Houk, K. N. *J. Am. Chem. Soc.* **1987**, 109, 3698.

TABLE 2. Energy Changes Calculated for the Intramolecular Catalysis of Z-Substituted Phenyl Maleate Esters in the Gas Phase^a

Z	pK _a ^b	HF/6-311+G*			B3LYP/6-311+G*
		ΔE ₁ ^c kcal/mol	ΔE ₂ ^d kcal/mol	ΔE ₃ ^e kcal/mol	ΔE ₃ ^e kcal/mol
<i>p</i> -CH ₃	10.26	12.29	-0.10	17.53	7.8
H	9.88	11.98	-0.18	16.71	7.4
<i>p</i> -Cl	9.38	11.20	-0.45	14.59	5.7
<i>m</i> -Cl	9.03	10.85	-0.52	14.15	5.0

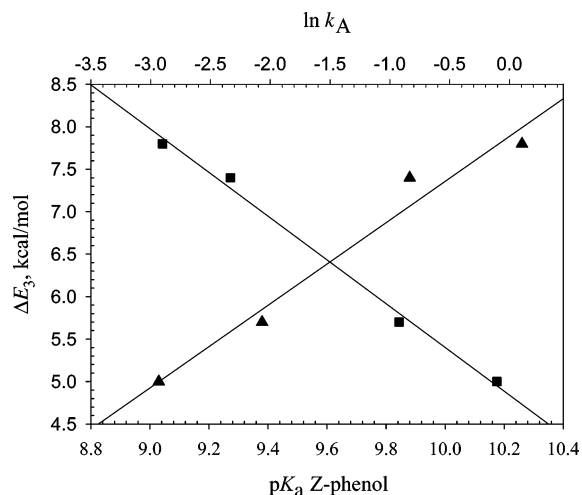
^a Values informed with zero point correction. ^b Values of the pK_a of the leaving phenol taken from ref 33. ^c Energy difference between TS1 and the NAC structure ($E_{TS1} - E_{NAC}$). ^d Energy difference between TI and TS1 ($E_{TI} - E_{TS1}$). ^e Energy difference between TS2 and NAC ($E_{TS2} - E_{NAC}$).

path toward reactants was followed starting at the geometry of TS2 by shortening the C₈–O₁₀ ester bond distance. By this inspection, only a shoulder is observed at the TS1 and TI zone. These results are not surprising considering the small values of the difference in energy between TS1 and TI, ΔE₂, (at most 0.52 kcal/mol) which show that TI is only slightly more stable than TS1 for all the substrates studied.

The topology of this gas-phase potential surface compares well with the one obtained for the *p*-methyl derivative evaluated with B3LYP/6-311+G* and full geometry optimization within a continuum solvent model with water as solvent. By this methodology, the NAC approach geometry was located as a minimum of the potential surface at an O₂–C₈ distance of 2.53 Å, with the O₂C₈O₉ angle of 100°. No TI could be found starting from this NAC by a careful O₂–C₈ distance approximation scan search. Instead, the energy continuously raises until an energy shoulder is reached between 1.676 and 1.576 Å; these points being 16.98 and 17.11 kcal/mol higher in energy, respectively, than the NAC structure. An activation energy for *p*-methylphenoxide departure from NAC of 23.01 kcal/mol is evaluated with this methodology; the TS2 being located at a C₈–O₁₀ distance of 2.117 Å.

Further evaluation of the intermediate existence was performed with B3LYP/6-31+G* by inclusion of six discrete water molecules distributed around relevant centers of negative charge localization, as determined from the electrostatic potential map obtained under the continuum solvent model (Figure S10). The number of water molecules was chosen in such a way as to assist the negative-charge evolution along the formation and/or fragmentation of the suspected TI. In doing so, we considered it adequate to solvate the oxygen negative center of the putative TI (one water molecule added at this site) and each of the negative oxygens in the open ester (one water molecule at each site). Two extra water molecules were added to avoid mutual electrostatic interactions between the water molecules more directly involved with the reacting centers along the coordinate. The sixth water molecule was added to stabilize the oxygen of the phenoxide group and proved not to be involved along the inspected coordinate, as it ended up at the carboxylate group. Under this approach, a flat region on the potential-energy surface at an O₂–C₈ distance of 1.63–1.72 Å was found from which the NAC minimum is reached without energy cost (Figure S11).

The gas-phase computational results for the difference in energy between the TS2 and the NAC structure, ΔE₃ (B3LYP/6-311+G*), were plotted as a function of the pK_a of the substituted phenol leaving group, giving a good linear relationship (Figure 1), with a slope of 2.37 ($r^2 = 0.97$). From this

**FIGURE 1.** Brønsted-type plot of the energy for the transition state of the rate-limiting step vs the pK_a of the leaving group. (▲) Relationship between rate constants for the anhydride formation for aryl maleate esters and the energy for the transition state of the rate-limiting step (■).

value, a computational value⁵⁹ of β_{lg} of -1.03 can be calculated in excellent agreement with the experimentally determined value (see above). In addition, a good linear relationship with slope of -1.04 ($r^2 = 0.994$) was obtained between ΔE₃ (B3LYP/6-311+G*) and ln k_A (Figure 1), which shows the consistency between the kinetics and the theoretical results, despite the fact that the theoretical calculations pertain to the reaction in the gas phase. This result is not unexpected because the solvent effect should affect the reaction of the whole series in a proportional way.

Mulliken natural population analysis on the oxygen atom of the leaving groups at the transition state (TS2) determined from the theoretical calculations did not show an appreciable change for the different substrates because the values are between -0.54 and -0.58 (-0.56 for the *p*-methyl derivative in a water continuum; Figure 2). These values are remarkably similar to the values obtained from linear free-energy relationships, determined from experimental data (see above).

Conclusions

The experimental values of β_{lg} and β_{Eq}, obtained for the reaction, are consistent with a mechanism that involves ester C–O bond breaking in the transition state of the rate-determining step. This point was successfully correlated with theoretical results where the bond length was determined in the range of 1.806–1.829 Å in the transition state in the gas phase and 2.117 Å in solution.

Moreover, the estimated charge on the oxygen leaving group in the transition state of the rate-determining step estimated from experimental data was -0.44 ± 0.10, in excellent agreement with the theoretical results that yield values between -0.54 and -0.58. Finally, we would like to remark on the small ΔE observed between TI and TS1 obtained by HF/6-311+G* as well as the flatness of the potential energy surface on this region

(59) This value is calculated dividing the slope of Figure 2 by 2.3, because the energy is related to the natural logarithm of the rate constant, and the Brønsted plots are drawn using the logarithm of the rate constant

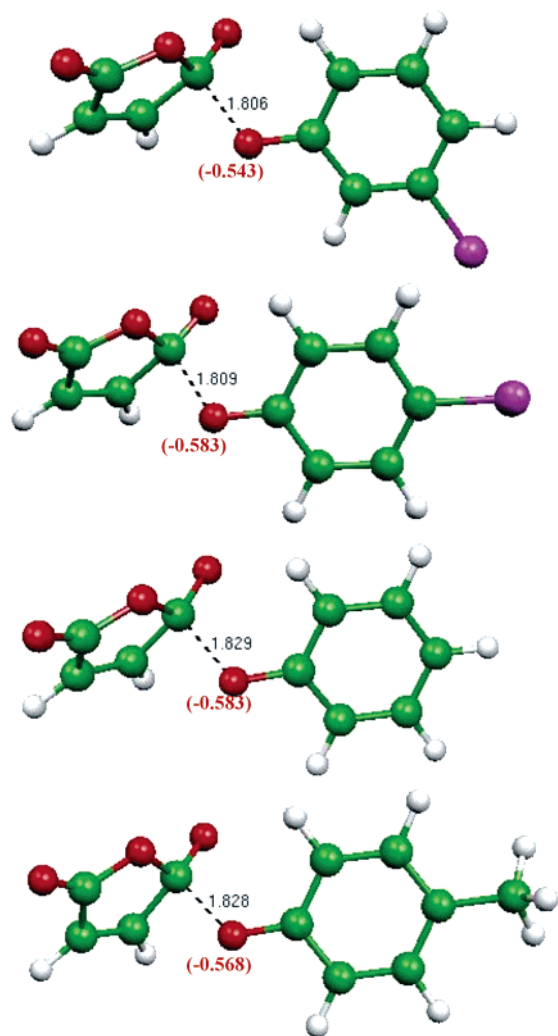


FIGURE 2. Optimized structure for the rate-limiting transition state of aryl maleates intramolecular hydrolysis obtained from DFT (B3LYP/6-311+G*).

when B3LYP calculations are performed either under a continuum solvent model or with a discrete number of water molecules. This theoretical profile seems to indicate that if the intermediate is formed it will have a considerably short lifetime due to its low activation energy to revert to reactants. The theoretical results do not give unequivocal proof for a concerted or stepwise mechanism, but they rather support a borderline situation. On the other hand, based on the similarities found in the behavior of this system when compared with others that are known to react by concerted mechanisms, we suggest that an enforced concerted mechanism is the most appropriate to describe these reactions.

Experimental Section

Materials. The monoaryl hydrogen maleate esters were prepared from maleic anhydride and the appropriate phenol, adapting the method described in the literature.⁶⁰ The products were characterized by IR and NMR (¹³C and ¹H), as in previous work.⁴¹ Maleic

anhydride was sublimed before use.⁶¹ The purity of the products was also checked by comparing the UV–visible absorption spectrum of a solution of the ester fully hydrolyzed with a mock solution containing maleic acid and the corresponding phenol.

Aqueous solutions were made up from water purified in a Millipore apparatus. Acetonitrile HPLC grade was dried on silica gel 10% p/v, as described in the literature.⁶¹ It is very important to have the solvent dried because, with traces of water, the substrate hydrolyzes before the solution can be used.

Kinetic Procedures. Most reactions were carried out in a stopped flow apparatus (SF) with unequal mixing syringes. The appropriate ester dissolved in dry acetonitrile was placed in the smaller syringe (0.1 mL). The large syringe (2.5 mL) was filled with water containing all the other ingredients. The total acetonitrile concentration was 3.85% v/v. The solution of the substrate for the kinetic determinations was freshly prepared in dry acetonitrile in the appropriate concentration to get a final concentration of 1.2×10^{-4} M.

All reactions were run at 25.0 ± 0.1 °C at constant ionic strength (0.5 M) using NaCl as the compensating electrolyte. The pH measurements were done in a pH meter at controlled temperature and calibrated with buffers prepared according to the literature.⁶²

The observed rate constants were determined by measuring the change in absorbance at 250 or 265 nm, depending on the ester. In some of the experiments, the pH of the solution was checked after the reaction by measuring it in the discarded solution, and the changes observed were always less than 0.03 pH units. The kinetic traces were fitted with one exponential equation using the SF apparatus's software. The p*K*_as of substituted phenols were taken from literature.⁶³

Computational Procedures. All calculations were performed with the Gaussian 98 package of programs.⁶⁴ The geometry of all stationary points was fully optimized. The most stable structures found are in good agreement with the NAC.¹¹ The potential energy surface from the NAC to the TI and from this intermediate to the products, formed by the departure of the phenoxide group, were followed by choosing appropriate distinguished reaction coordinates. The geometries of the B3LYP/6-311+G* stationary points were obtained by the full re-optimization of the HF/6-311+G* structures. The energies obtained within the continuum solvent model were calculated with full geometry optimization using the Jaguar program.⁶⁵ The model solvent used was water (dielectric constant = 80.370, density = 0.99823 g/mL) within the continuing model implemented in Jaguar.⁶⁶ The B3LYP/6-31+G* calculations, including six water molecules, were performed with full geometry

(61) Perrin, D. D.; Armarego, W. L. G. *Purification of Laboratory Chemicals*, 3rd ed.; Butterworth-Heinemann, Ltd: Oxford, U.K., 1994.

(62) *Handbook of Chemistry and Physics*, 72nd edition; Lide, D. R., Ed.; CRC Press: Boca Raton, FL, 1991–1992; pp 8-30–8-35.

(63) Jencks, W. P.; Regenstein, J. *Handbook of Biochemistry and Molecular Biology*, 3rd edition; CRC Press: Cleveland, Ohio, 1977.

(64) Frisch, M. J.; Trucks, G. W.; Schlegel, H. B.; Scuseria, G. E.; Robb, M. A.; Cheeseman, J. R.; Zakrzewski, V. G.; Montgomery, J. A., Jr.; Stratmann, R. E.; Burant, J. C.; Dapprich, S.; Millam, J. M.; Daniels, A. D.; Kudin, K. N.; Strain, M. C.; Farkas, O.; Tomasi, J.; Barone, V.; Cossi, M.; Cammi, R.; Mennucci, B.; Pomelli, C.; Adamo, C.; Clifford, S.; Ochterski, J.; Petersson, G. A.; Ayala, P. Y.; Cui, Q.; Morokuma, K.; Malick, D. K.; Rabuck, A. D.; Raghavachari, K.; Foresman, J. B.; Cioslowski, J.; Ortiz, J. V.; Stefanov, B. B.; Liu, G.; Liashenko, A.; Piskorz, P.; Komaromi, I.; Gomperts, R.; Martin, R. L.; Fox, D. J.; Keith, T.; Al-Laham, M. A.; Peng, C. Y.; Nanayakkara, A.; Gonzalez, C.; Challacombe, M.; Gill, P. M. W.; Johnson, B. G.; Chen, W.; Wong, M. W.; Andres, J. L.; Head-Gordon, M.; Replogle, E. S.; Pople, J. A. *Gaussian 98*, revision A.7; Gaussian, Inc.: Pittsburgh, PA, 1998.

(65) *Jaguar* version 6.0, Schrodinger, LLC, New York, NY, 2005. See: <http://www.schrodinger.com>.

(66) (a) Tannor, D. J.; Marten, B.; Murphy, R.; Friesner, R. A. Sitkoff, D.; Nicholls, A.; Ringnalda, M.; Goddard, W. A.; Honig, B. *J. Am. Chem. Soc.* **1994**, *116*, 11875. (b) Marten, B.; Kim, K.; Cortis, C.; Friesner, R. A.; Murphy, R. B.; Ringnalda, M. N.; Sitkoff, D.; Honig, B. *J. Phys. Chem.* **1996**, *100*, 11775.

(60) Bojanowska, I.; Jasinski, T. *Pol. J. Chem.* **1989**, *63*, 455.

optimization for each O₂–C₈ fixed distance. The characterization of stationary points was done as usual by Hessian matrix calculation, proving all eigenvalues are positive for a minimum and only one eigenvalue is negative for a transition state. In the gas phase, the connectivity between the stationary points was established by intrinsic reaction coordinate calculations.⁶⁷

Acknowledgment. This research was supported in part by the Consejo Nacional de Investigaciones Científicas y Técnicas (CONICET), the Agencia Córdoba Ciencia, Agencia Nacional de Ciencia y Tecnología (FONCYT), and the Universidad

Nacional de Córdoba, Argentina. G.O.A. is the grateful recipient of a fellowship from CONICET.

Supporting Information Available: Rate constants for the anhydride formation, effect of pH and buffer concentration, B3LYP/6–311+G* normal frequencies for TS2 and related theoretical data, absorbance vs time for the *p*-chlorophenyl hydrogen maleate hydrolysis, plot of τ_1^{-1} as a function of pH, and linear free relationship plots. This material is available free of charge via the Internet at <http://pubs.acs.org>.

JO061165E

(67) Gonzalez, C.; Schlegel, H. B. *J. Phys. Chem.* **1990**, *94*, 5523.